Molecular Crystals and Liquid Crystals

Publication details, including instructions for authors and subscription information:
http://www.tandfonline.com/loi/gmcl20

C60 Aggregates in Pyrrolidine and N-Methyl-2-Pyrrolidinone Evidenced by Surface-Enhanced Raman Scaterring Spectra

M. Baibarac [a], N. Preda [a], L. Mihut [a], T. Velula [a], I. Baltog* [a], J. Y. Mevellec [b] & S. Lefrant [b]

[a] Lab. 160, National Institute for Physics of Materials, Bucharest, Romania

[b] Lab. de Physique Cristalline, Institut des Materiaux de Nantes, 2 Rue de la Houssiniere, Nantes, France

Version of record first published: 18 Oct 2010

To cite this article: M. Baibarac, N. Preda, L. Mihut, T. Velula, I. Baltog*, J. Y. Mevellec & S. Lefrant (2004): C60 Aggregates in Pyrrolidine and N-Methyl-2-Pyrrolidinone Evidenced by Surface-Enhanced Raman Scaterring Spectra, Molecular Crystals and Liquid Crystals, 417:1, 87-103

To link to this article: http://dx.doi.org/10.1080/15421400490478434

Mol. Cryst. Liq. Cryst., Vol. 417, pp. 87/[571]–103/[587], 2004

ISSN: 1542-1406 print/1563-5287 online
DOI: 10.1080/15421400490478434

Taylor & Francis
Taylor & Francis Group

C_{60} AGGREGATES IN PYRROLIDINE AND N-METHYL-2-PYRROLIDINONE EVIDENCED BY SURFACE-ENHANCED RAMAN SCATERRING SPECTRA

*M. Baibarac, N. Preda, L. Mihut, T. Velula, and I. Baltog**
National Institute for Physics of Materials, Lab. 160, Bucharest, P.O. Box MG-7, R-76900, Romania

J. Y. Mevellec and S. Lefrant
Institut des Materiaux de Nantes, Lab. de Physique Cristalline, 2 Rue de la Houssiniere, B.P. 32229, 44322 Nantes, France

At room temperature, soluted C_{60} in pyrrolidine and N-methyl-2-pyrrolidinone associates slowly in stable aggregates. The process originates in the charge transfer from the solvent molecules as electron donors towards fullerene. In the aggregate phase the intermolecular interactions lead to a large reduction in parent I_h C_{60} symmetry such that a modified phonon spectrum is observed. Using the surface-enhanced Raman scattering we demonstrate that the Raman range below 800 cm^{-1} is most diagnostic for aggregate assignment. In particular, the strong decrease of the radial breathing mode and appearance of new bands at 110 and 93 cm^{-1} due to the interball interactions must be noticed.

Keywords: aggregates; fullerene; SERS spectra

1. INTRODUCTION

At room temperature, solute C_{60} in single solvents like n-pentane, carbon disulphide, benzene, carbon tetrachloride etc. aggregates slowly in nanometer size clusters [1–6]. Whole process bases on weak intermolecular

This work was performed in the frame of the Scientific Cooperation between the Laboratory of Crystalline Physics of the Institute of Materials, Nantes, and the Laboratory of Optics and Spectroscopy of the National Institute of Materials Physics, Bucharest. The Institute des Materiaux de Nantes is part of the "Ecole Polytechnique de l'Universite de Nantes" and Unite Mixte de recherche CNRS-Universite de Nantes No.6502.

*Corresponding author. Tel.: +40-21-4930195, Fax: +40-21-4930267, E-mail: ibaltog@alpha2.infim.ro

interactions forces which determines the stability and the aggregated size. In general, these formations are very unstable even to the stirring or mechanical shaking of solution [7]. In binary liquid mixtures, consisting by a strong and a poor fullerene solvent, the aggregates form quickly and they are much more stable to mechanical disturbances [3]. Modification of the liquid mixtures and fullerene concentration induce important solvatochromic changes in the solution of C_{60} [3,6,8]. Another class of aggregates originates in the mild electrophylic character of C_{60}. In solvents with nucleophilic properties are formed, by charge transfer from the solvent molecules as electron donors towards fullerene, complexes which later on associate in stable aggregates likened to a crystalline network. A special attention was paid to the complexes of C_{60} with various aliphatic [9] and aromatic amines [10,11]. In this context, the pyrrolidine (P) and N-methyl-2-pyrrolidinone (NMP) which act both as solvent and as a reactant are particularly interesting. Due to the unpaired electrons of the nitrogen atom belonging to the amino and amide group this solvents have an increased chemical reactivity. Competition between nucleophilic addition and charge transfer favors the bonding of solvent molecules at the C_{60} cage, forming a functionalized fullerene which on associates in stable aggregates. Oneself arrangement of C_{60} in nanometer size clusters is a result of the environmental interactions which lead to variations of the phonon spectrum.

This can be investigated by Raman spectroscopy, one of the widest used techniques for characterizing and understanding of the properties of the fullerenes. A comparison between the Raman spectra of the aggregates of C_{60} in single solvents as toluene, benzene, *o*-dichlorobenzene ($C_6H_4Cl_2$) where act weak van der Waals forces and in solvents as P and NMP where act stronger forces of chemical origin is an inciting research subject. So far, such Raman studies were not reported. In this achievement an impediment is the measuring of very weak Raman signals as result of the fact that one must use samples in form of thin films which preserve better the aggregates formed in the solutions of C_{60}. Difficulty is surpassed in this paper using the surface-enhanced Raman scattering (SERS) as appropriate experimental method, which operating with enhanced Raman signals due to the resonant excitation of surface plasmons (Sps) [12,13] permits the investigation of a thin films of nanometric thickness.

In this context we note that very few SERS studies of C_{60} were reported and no one devoted to the aggregates of fullerenes [14–17].

2. EXPERIMENTAL

The solvents, toluene (T), *o*-dichlorobenzene (DCB), pyrrolidine (P) and N-methyl 2-pyrrolidinone (NMP), and C_{60} powder used in this work were

of Merck quality. One used solutions with the concentration of C_{60} in the range of 0.2–2 mg/ml. SERS spectra were performed at room temperature in ambient air in a backscattering geometry under excitation wavelengths at 1064 nm using a FT Raman Bruker RFS 100 spectrophotometer. Films of ∼100 nm thickness were obtained by the solvent evaporation on Au and Ag supports with a rough microstructure in the range of 10–100 nm. The preference for 1064 nm as Raman excitation wavelengths and Au as metallic support was dictated by the fact that the films of C_{60}, regardless the aggregation state showed a strong photoluminescence under visible excitation and the gold is more efficient SERS substrate at this excitation wavelengths.

Special care was paid to identify and separate the modifications of the SERS spectra due to the roughness and type of the metal substrate [18].

3. RESULTS AND DISCUSSION

It is well known that the SERS originates in two basic enhancement mechanisms: i) electromagnetic, resulted from the resonant excitation of the surface plasmons and ii) chemical, mainly due to charge transfer processes between the metallic substrate and adsorbed molecules. The intensity of the Raman emission excited by surface plasmons depends on the dielectric constant of the metal substrate [12,13] and for the visible range the silver and gold, which possesses the lowest absorption coefficients [19], are the most effective metallic supports. This fact becomes important in SERS spectroscopy of fullerenes, which are known as molecules with high chemical reactivity, readily forming charge-transfer compounds with metals as donors [20]. In this sense Ag and Au can be such donors, so that the SERS spectra should reveal significant differences in comparison with regular Raman spectra of C_{60} powder. In these circumstances for the use of SERS spectroscopy as suitable technique in the study of the C_{60} aggregates is necessary a correct evaluation of the support effect. This could be the explanation why so far were reported very few data concerning the variations of the C_{60} SERS spectra as function of the type of metal substrate [14–16,18] and no one relating the C_{60} aggregates.

A complete picture of the variation of C_{60} SERS spectra with the support roughness and the type of metal substrate is given in the Figure 1.

The resonant excitation of the Sps is achieved using as optical coupler a rough metallic substrate with a roughness in the range 10–100 nm. This process being independent of the chemical reactivity of the two adjacent media, a Raman spectrum excited by SPs should not differ from a regular one. In reality, the SERS spectra show frequently significant differences which are due to charge transfer processes taking place between the

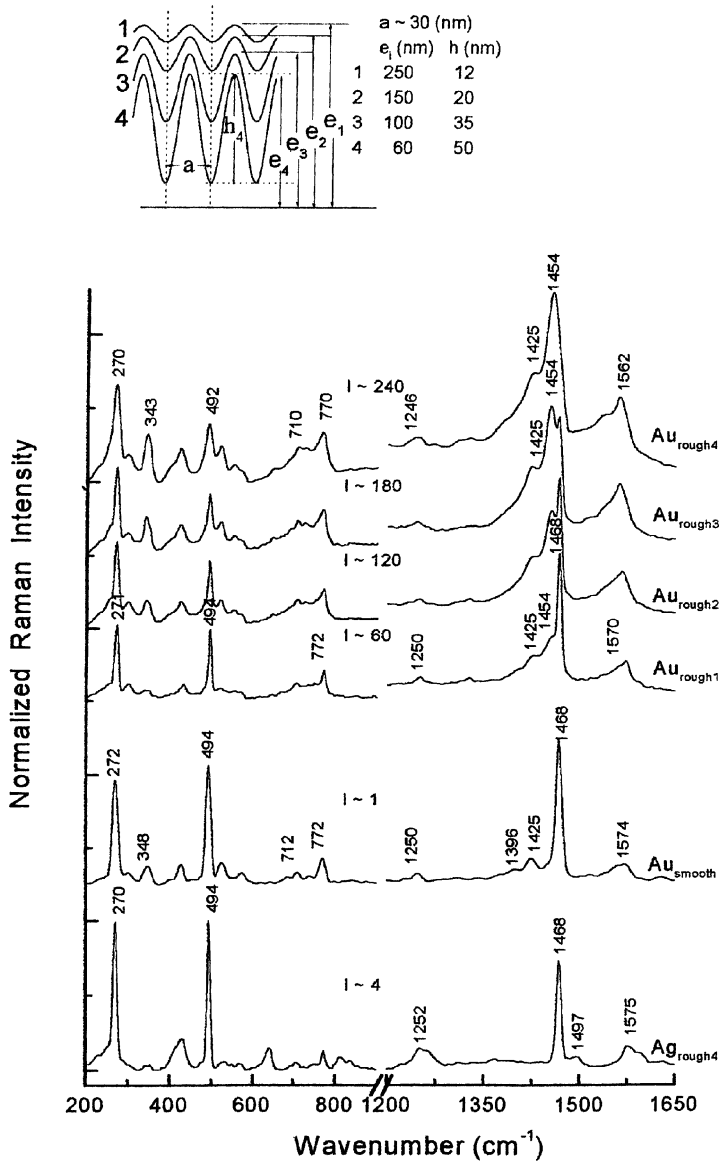

FIGURE 1 SERS spectra at $\lambda_{exc} = 1064$ nm of C_{60} as function of roughness and the type of metal substrate. In inset is illustrate idealized rough profiles defined by the thickness of the metallic film (e) and roughness parameter (h/a). All spectra were recorded on C_{60} films of ca. 100 nm thickness deposited by evaporation of the solvent (toluene).

metallic substrate and adsorbed molecules. These interface reactions, forming so called the chemical component in the SERS generation, plays an important role. Their dependence of the morphology of the metal substrate relate different adsorption mechanisms.

From the SERS perspective an active rough surface may be likened to a bird's-eye view of a multitude of columns of nearly the same diameter. It can described in terms of two quantities: a and h, the diameter and average height of these columns, respectively. In a former paper we have shown that using a diffraction grating as optical coupler the SERS intensity depends on the ratio between grating groove depth and grating periodicity [20]. Idealizing this picture, the rough surfaces of Au and Ag used as SERS supports could be assimilate with two-dimensional diffraction gratings. In this case, the roughness ratio, h/a, may be likened to a grating groove depth/grating periodicity ratio and any change in the h/a value should be accompanied by a specific variation of the SERS intensity. On the Figure 1, the inset illustrates different roughness obtained changing the evaporation conditions i.e. keeping the atomic beam at a constant grazing incidence to the target surface and changing the amount of evaporated metal. In this way one prepared four types of rough metallic surfaces whose parameters h and h/a were estimated by scanning tunneling microscopy (STM). A semi-quantitative the comparison of the Raman spectra measured on supports with different roughness was obtained using a normalized scale and taking as unit the Raman signal of C_{60} film deposited on the smooth substrate of Au and the Raman spectrum of sulfur as standard.

The variation of the SERS spectra as function of the metal substrate and surface roughness is presented also in Figure 1. SERS spectra recorded on Au and Ag supports bring to view all Raman active modes in C_{60}, i.e. two A_g and eight H_g modes [21] and the influence of the metal substrate is noticed by the different magnitude of the measured Raman signal and the appearance of new bands. One see easily that the gold is a more efficient SERS substrate at excitation wavelengths of 1064 nm. Variation of the Raman intensity with the support roughness, shown in Figure 1 by the spectra $Au_{rough1} - Au_{rough4}$, relates the efficiency of surface plasmons excitation with the increase of the h/a parameter. The chemical mechanism, contributing to the SERS process, relates the different records on Au and Ag substrate. Figure 1 shows clearly that the gold support is chemical more reactive and the band peaking at ca. 343 cm^{-1} is revealing.

The different chemical behavior of the Au and Ag supports is due to the interposition of an intermediate compound layer between the C_{60} molecules and metal substrate formed during in air manipulation. Ag has a strong oxidation tendency to form a stable compound Ag_2O, which as a surface layer prevents the direct interaction between C_{60} and metal substrate. In this case the SERS spectrum is similar to the regular Raman spectrum

recorded on C_{60} powder. For the gold, which is the only metal that shows no direct reaction with oxygen, even at high temperature, the lack of a covering oxide layer permits a direct interaction, of charge-transfer type, with adsorbed fullerenes. In this case thinking of a compound as Au_xC_{60}, analog with the alkali metal-doped fullerenes like M_3C_{60} (M = K, Rb, etc.), one can explain similarly the down shift of the Raman band associated to the pentagonal pinch mode $A_g(2)$. Besides, the experimental data show that the position and the profile of the $A_g(2)$ band depend of the roughness of the substrate. With the increase of the substrate roughness, the $A_g(2)$ band get a more asymmetric profile in its lower energy side formed by the growth of three bands at 1454, 1425 and 1390 cm^{-1}. At the first sight this kind variation seems normal, a greater roughness meaning a greater reacting surface, i.e. an increased contribution of the chemical component in SERS generation. However, using supports of different roughness, the SERS spectra presented into normalizes scale are not identical if the enhancement should depend only of the efficiency of the surface plasmons excitation. Another process can be a charge transfer activated by the incident excitation light. In this case an electron of the metal, excited by the incident photon, tunneling into excited state of the adsorbed C_{60} induces in this a different equilibrium geometry. The return of the electron to the metal, leaves fullerene into another vibration excited state than neutral molecule which will lead to emission of a Raman-shifted phonon. In this case the different SERS spectrum results from the activation of forbidden transitions in the high icosahedral (I_h) symmetry of the isolated C_{60} by a lowering-symmetry effect. Thus, the bands at 343 and 1562 cm^{-1} may be attributed to the odd-parity mode $H_u(1)$ and $H_u(7)$, respectively.

Aggregation of the fullerenes in single solvents is a typical example of weak intermolecular interactions. Based on van der Waals forces this property relates the polarizability of the interacting particles and its magnitude determines the stability and the size of aggregates. An example is the aggregation of C_{60} in a polar solvent as *o*-dichlorobenzene achieved if the solution is left standing a long period of time, Figure 2. It exhibit the modifications of the SERS spectra of C_{60} due both to the interactions of fullerenes with the gold substrate and its aggregation. As above, the substrate effect consisting in the presence of a band at 342 cm^{-1} and in the shift of the $A_g(2)$ band at about 1458 cm^{-1} was observed mainly on films prepared from the fresh solutions.

The most indicative for the fullerenes aggregation there is in the spectral range below 800 cm^{-1} and as general feature one can mention the strong decrease of the Raman bands associated to the radial vibration modes.

Aggregation leads to a distortion of the molecule and a large reduction in symmetry such that many previously forbidden line appear in the IR and

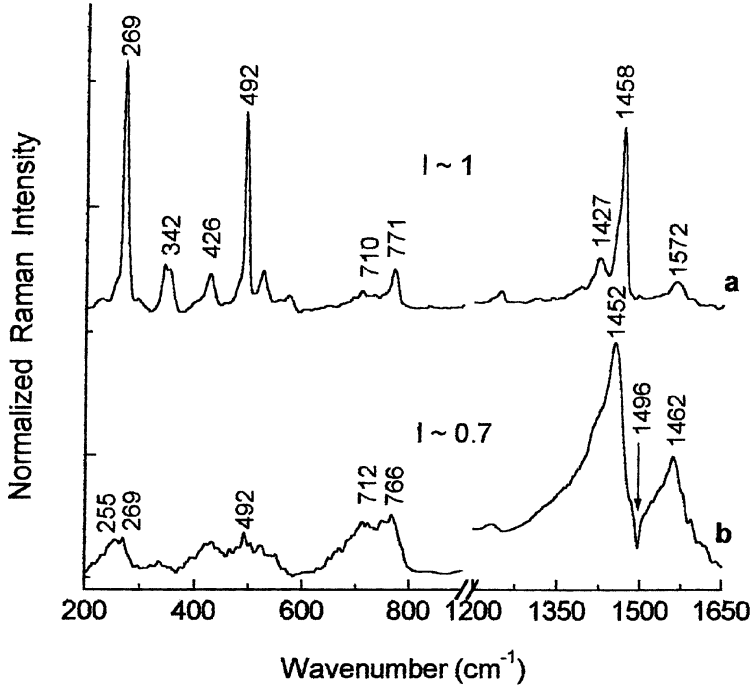

FIGURE 2 Aggregates of C_{60} in *o*-dichlorobenzene evidenced by the SERS spectroscopy at $\lambda_{exc} = 1064$ nm on films of ca. 100 nm thickness deposited on Au support . Spectra **a** and **b** were recorded on films prepared from fresh solution and left standing in the dark at ambient temperature for 12 days, respectively.

Raman spectra of the agregate. The reduction in symmetry leads also to a multiple splitting of some allowed Raman and IR modes of C_{60} and new bands appear while the intensity of many original bands decreases. In this sense we notice the weak band at $\sim 255\,cm^{-1}$ which seems appearing as one component resulted from the splitting of the $H_g(1)$ band of the I_hC_{60} into three components at 275, ~ 254 and $\sim 242\,cm^{-1}$ in the C_{60} dimer [22]. Asymmetrization towards low energy side of the $A_g(2)$ band and replacing of the $H_g(8)$ line with a wide band at $\sim 1562\,cm^{-1}$ is also a consequence of the lowering symmetry effect, typical when C_{60} associates through polymerization [23], coalescence under light irradiation [17] or pressure-polymerization [24].

Another class of aggregates are those formed in liquids with nucleophilic properties as pyrrolidine (P) and N-methyl-2-pyrrolidinone (NMP) which act both as solvent and as a reactant. In this case the aggregation of C_{60} is driven by stronger intermolecular interactions forces. By charge transfer

from the solvent molecules as electron donors towards fullerene are formed complexes, which later on associate in stable aggregates likened to a crystalline network.

Figures 3a and 3b show the SERS spectra of films prepared from solutions of C_{60} in pyrrolidine. It is striking the difference between the two figures which correspond to the films prepared from: i) fresh solutions, i.e. just after the dissolving of fullerene, and ii) the solutions left standing for 34 days. Figure 3a shows that in the initial state the SERS spectra exhibit remarkable similarities. This indicates a strong interaction with the molecules of pyrrolidine and the formation of molecular complexes whose physical and chemical properties are different in comparison with parent fullerene. Due to the lowering of the high icosahedral (I_h) symmetry of C_{60}, resulted from the bonding of pyrrolidine molecule on the C_{60} cage are activated both the silent and high order vibrations modes which become observable both in the IR absorption spectra and Raman spectra. In this sense it is relevant the appearance in the Figure 3a of the band at $1500\,cm^{-1}$ close of that observed at $1497\,cm^{-1}$ in the IR absorption spectra of the $C_{60}{\cdot}4C_6H_6$, $C_{60}{\cdot}xCCl_4$, $C_{60}{\cdot}1.5CS_2$, $C_{60}{\cdot}C_2HCl_3$ clathrates [25]. Besides, the lines at 134 and $257\,cm^{-1}$ and the enhancement of the bands group ranging 650–$750\,cm^{-1}$, all reported as due to the coupling between two balls [23,26], indicate a strong process of association of the molecular complexes $C_{60}P$, which takes place very in the begining; after the dissolving of fullerenes. This explains also the absence of the band at $342\,cm^{-1}$, evidence of the isolated C_{60} which can interacts with the gold substrate.

By aggregation of C_{60} the SERS spectra change continously and stabilize after different storing time of the preparing solutions. As function of fullerenes concentration the SERS spectra no more vary after few days and few weeks for the concentration of 0.2% wt and 0.05% wt, respectively. All spectra show new bands in the ranges of 1200–1350 and 2500–$3500\,cm^{-1}$. Spectrum 1 in Figure 3b is fully relevant, it is almost identical with the SERS spectrum of the amorphous carbon. On the other hand, spectra 2 and 3 from Figure 3b, exhibit two bands at $\sim$1585 and $\sim 1300\,cm^{-1}$ as a rule omnipresent in the graphitic materials; the former is attributed to the tangential stretching modes and the latter is known as D band relating of disorder state and defect [21].

The appearance of SERS spectrum similar to the amorphous carbon may result from the destroying of the fullerene by the successive reactions with pyrolidine molecules. If such a process really occurs then it must be more efficient in the less concentrated solutions, i.e. when the number of solvent molecules allocated to the one molecule of C_{60} is greater. Nevertheless, the spectra from Figure 3b show a variation contrary to expectation, the mark of the amorphous carbon is rather found on sample prepared from the more concentrated solution. Another explanation makes reference to the

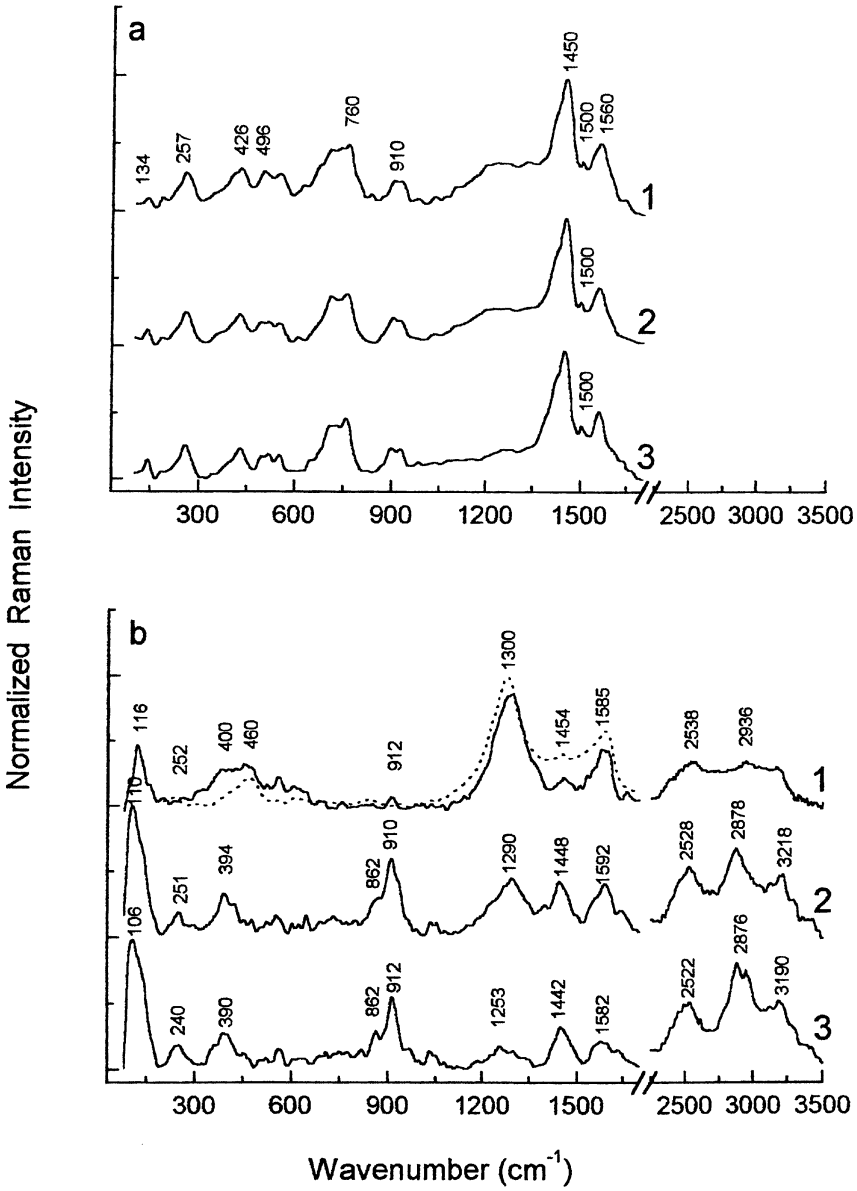

FIGURE 3 Aggregates of C_{60} in pyrrolidine evidenced by the SERS spectroscopy at $\lambda_{exc} = 1064$ nm on films of ca. 100 nm thickness deposited on Au support . Spectra 1, 2 and 3 were recorded on films prepared from solution of concentration 0.2, 0.1 and 0.05%wt, respectively. Figure **a** corresponds to the initial state, i.e. when one used films prepared from fresh solution and **b** to the aggregated phase formed in the solution left standing in the dark at ambiental temperature for 34 days.

aggregation of the functionalized fullerenes in three dimensional structures. The analogy with a crystallization process taking place into saturated solutions explains the dependence of concentration solutions; the higher concentration advantages a rapid crystallization and the formation of disordered aggregates while in the solution of lower concentration the aggregation proceeds slowly leading to three-dimensional structures resembling to a crystalline lattice. With this scenario, the presence of the Raman bands at 1585, 1450 and 1300 cm^{-1}, the last appearing as D band, have a specific meaning. The D band occurs normally in powdered and randomly oriented crystalline graphite, glassy carbon, highly ordered pyrolitic graphite, carbon nanotubes and amorphous carbon [21]. It is activated in the first order scattering process of sp^2 carbons by the presence of different defects (in-plan substitutional hetero-atoms, vacancies, grain boundaries) and by finite size effects, all these lowering the symmetry of the quasi-infinite graphite lattice. On the basis of size effect [27], the intensity of the D band becomes measuring for the inverse of the aggregate characteristic size.

Looking the aggregates as crystalline particles of different size and shape one expects specific effects in the radiation-matter interaction. In this sense, one of the most unusual properties of graphite is the activation of the second-order Raman spectrum whose intensity varies with the sizes of the crystalline domains [27–29]. Second-order Raman line, called overtone, originates in combined density of states of two phonons of equal and opposite nonzero wave vector, is located at approximately twice the frequency of the one-phonon density of states spectrum.

Such spectra are presented in the Figure 3b where one observes that the same as for others particles of graphite the main second-order Raman line concern the first order in the interval of 1000–1600 cm^{-1}. We consider this as a clear evidence for the formation of C_{60} aggregates likewise with crystalline lattice. Because the intensity of the second-order Raman spectrum relates the aggregates size, on the basis of spectra 2 and 3 from Figure 3, one infers that in the diluted solutions were formed aggregates of greater size.

Disparity between the strength of the intermolecular and intramolecular bonds divides the phonon spectrum of the aggregate into intermolecular and intramolecular vibrations. For the graphite particles the intermolecular vibrations are observed in the low-frequency of the Raman spectrum [23,26]. Based on this reasoning the band at about 110 cm^{-1} may be attributed to an interball vibration mode in analogy with the Raman lines associated to the covalent bonds between adjacent C_{60} in dimers [30–32].

Summarizing the data presented in Figure 3a and Figure 3b one infers two stages in the aggregation of C_{60} in pyrrolidine. In the beginning, as result of the fact that C_{60} is a good electron acceptor while P is a good electron donor, are formed C_{60}P charge transfer complexes. This interaction

explains the down-shift of the $A_g(2)$ band and the weakening of the $H_g(1)$ radial band. In addition, the new bands at 134 and 257 cm^{-1} suggest that the interaction between C_{60} and P lead also at C_{60} dimer. In the second stage, these molecular complexes associate slowly forming aggregates of different size resembling a crystalline network. The signature for this stage is done by the appearance of the band at $\sim$106–116 cm^{-1}, associated to the interball stretching and of second order Raman spectrum.

This process can be illustrated by the scheme 1.

If the reasoning is correct then the use of another nucleophile solvent must lead to similar results. An example is the aggregation of C_{60} in N-methyl-2-pyrrolidinone, Figure 4.

The same as above, the aggregated phase has been obtained leaving the solution of C_{60} to stand in the dark a long period of time. the modifications of the SERS spectra displayed in Figure 4 are the result of the interactions of C_{60} with the metallic substrate, with molecules of solvent and with neighbor

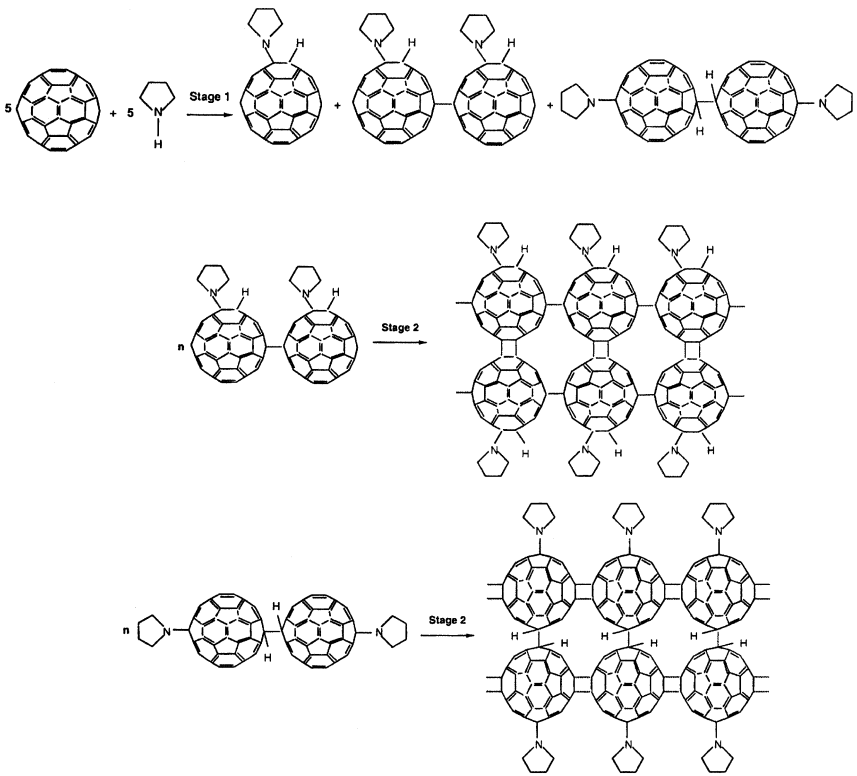

SCHEME 1

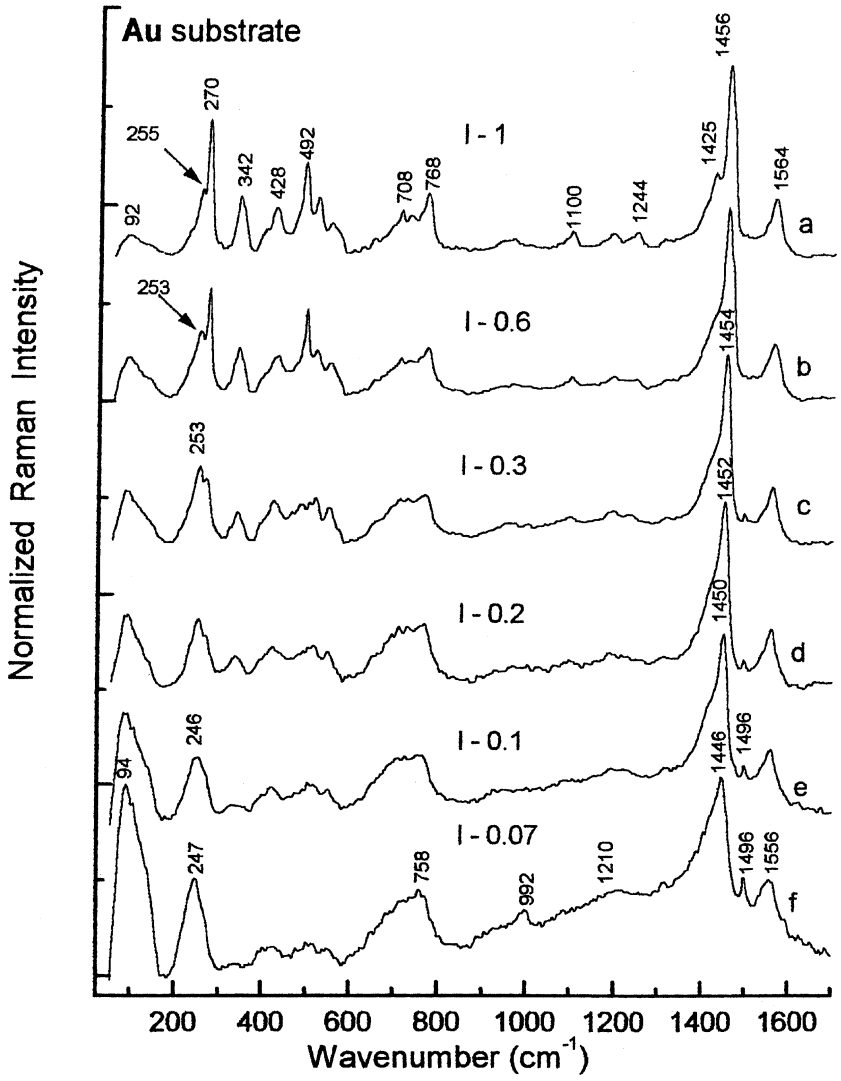

FIGURE 4 Aggregates of C_{60} in N-methyl-2-pyrrolidinone evidenced by the SERS spectroscopy at $\lambda_{exc} = 1064$ nm on films of ca. 100 nm thickness deposited on Au support. Spectrum **a** corresponds to the initial state, i.e. when one used film prepared from fresh solution and **b**, **c** **d**, **e** and **f** on films prepared from solution left standing in the dark at ambient temperature for 1, 3, 6, 18 and 34 days, respectively. The concentration of C_{60} was of 0.04% wt.

molecules which form the aggregates. They are closer of them relating the aggregation of C_{60} in DCB. An indicative is the progressive decreases of the band at $\sim 342\,cm^{-1}$ which signals the interaction of C_{60} with the metal substrate. In comparison with the aggregation of C_{60} in DCB we signal a greater decreasing of the measured Raman signal and the appearance of new bands peaking around of 1496, 250 and $94\,cm^{-1}$. As above, the charge transfer between the solvent molecule towards fullerene leads to the formation of stable complexes, which relate specific variations of the SERS spectra. the band at about $\sim 255\,cm^{-1}$ is the most relevant for the aggregation of C_{60} in NMP. It appears from the beginning as shoulder of the characteristic Raman band attributed to the $H_g(1)$ vibration mode of C_{60} in the icosahedral (I_h) symmetry. During the aggregation it grows and broadens tending to a Gaussian profile shifted at about $246\,cm^{-1}$ becoming one of the most important Raman band. This modification of position fits very well with the theoretical predictions regarding the splitting of the $H_g(1)$ band of the I_hC_{60} into three components at 275, ~ 254 and $\sim 242\,cm^{-1}$ in the C_{60} dimer [22]. In this case the new band at $\sim 246\,cm^{-1}$ could relate many cage of C_{60} associate in chain or network.

The same as in Figure 3 we disclose two steps in the aggregation of the C_{60} in NMP. In the beginning, just after the dissolving of fullerene, the molecules of solvent bonding on C_{60} form molecular complexes similar to functionalized fullerenes which by the successive associations form three-dimensional aggregates resembling with a crystalline network. The slower stage, which lasts longer time, is featured by a shift of these bands until 246 and $1446\,cm^{-1}$, respectively and the enhancement of another one around $94\,cm^{-1}$.

Whole process ends by the modification of the phonon spectrum concerning both the intramolecular and intermolecular vibrations. The former relates the decreasing of the high icosahedral (I_h) symmetry of C_{60} and the latter interball interactions. In this frame one explains the appearance of the band at $1496\,cm^{-1}$ as due to the combination modes $F_{1g}(2)\otimes F_{1u}(1)$ [25] activate C_{60} of lowered symmetry and at $\sim 94\,cm^{-1}$ associated to the interball stretching mode in analogy with the Raman lines associated with the covalent bonds between adjacent C_{60} in dimers [30–32]. This process can be illustrated by the scheme 2 which goes on in two steps.

4. CONCLUSIONS

This paper reports new results obtained by SERS spectroscopy concerning the aggregation of C_{60} in *o*-dichlorobenzene (DCB), pyrrolidine (P) and N-methyl-2-pyrrolidinone (NMP). For a correct evaluation of the variations SERS spectra due to the aggregation of C_{60} in different solvent, the

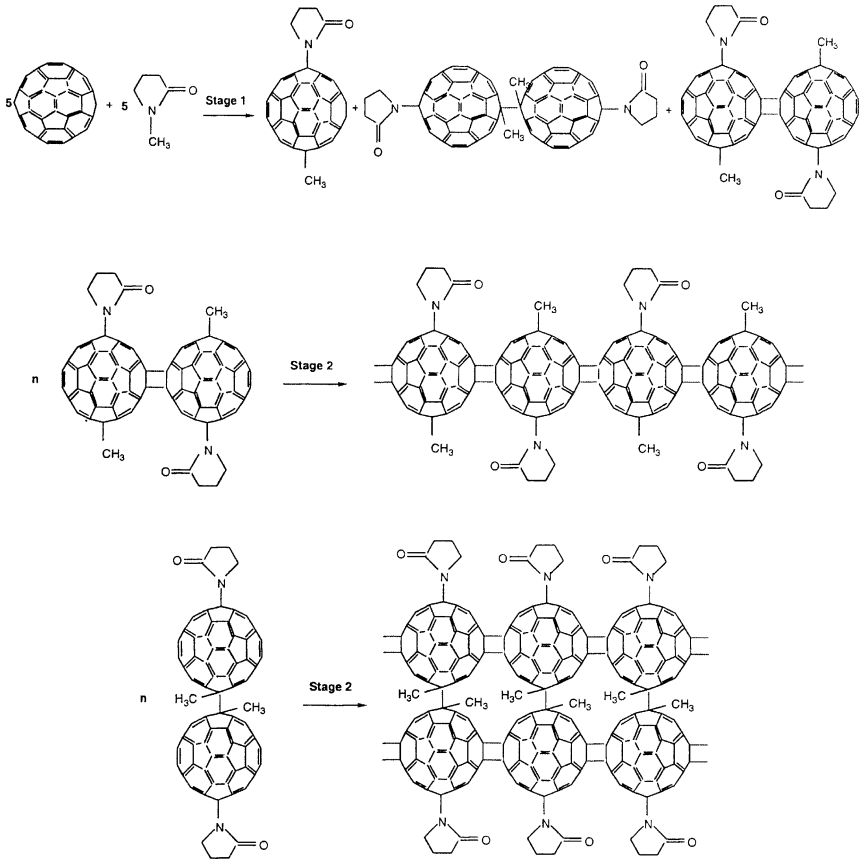

SCHEME 2

dependece of C_{60} SERS spectrum of type of metal substrate and surface roughness are also investigated.

The results can be summarized as follows:

i) The SERS spectra of the C_{60} film deposited on Ag and Au substrate with the same roughness are different. This is due to the interposition of an intermediate compound layer between C_{60} and metal substrate. Ag in air forms Ag_2O, as stable surface layer, which prevents the direct interaction between C_{60} and metal substrate. For the gold, the lack of a covering oxide layer permits a direct interaction, of charge-transfer type, with adsorbed fullerenes. The main evidence of the interaction between C_{60} and gold substrate is done by a new band at $\sim 342\,cm^{-1}$. It is explained in terms of a charge-transfer activated by the incident excitation light.

ii) The interface reactions, form so called the chemical component in SERS generation, depends also of the morphology of the metal substrate. We have demonstrated this using metallic supports of different roughness defined by the ratio h/a which, may be likened to a grating groove depth/grating periodicity ratio.

iii) Aggregation of C_{60} in DCB involves weak intermolecular interactions on the type van der Waals forces. The main SERS signature is done by: a) the weakening of the bands associated to radial vibration modes and b) down-shift and a strong asymmetry in the low energy side of the pentagonal pinch mode $A_g(2)$.

iv) Aggregation of C_{60} in pyrrolidine and N-methyl-2-pyrrolidinone is different as result of the fact that they act both as a reactant and as a solvent. In this case the aggregation process is driven by stronger forces originate in the charge transfer from the solvent molecules as electron donors towards fullerene. The aggregation develops in two stages: in the beginning are formed quickly by the charge-transfer molecular complexes as dimer of C_{60} which on associate slowly in stable aggregates. The Raman range below $800\,cm^{-1}$ is most diagnostic for aggregate assignment. In particular, the main indicative is the decreasing or even disappearance of the Raman bands associated to the radial vibration modes. We conclude that in NMP are obtained linear chains of C_{60} which in the SERS spectra are evidenced by the active Raman interball mode at $92\,cm^{-1}$ while in P are formed aggregates highly organized likewise crystalline network. These are signed in the SERS spectra by the Raman-active interball modes of C_{60} polymer chain two-dimensional tetragonal at 110–$118\,cm^{-1}$ and the appearance of a second order Raman spectrum.

REFERENCES

[1] Rouff, R. S., Malhorta, R., Huestis, D. L., Tes, D. S., & Lorents, D. (1993). *Nature*, *362*, 140.

[2] Ying, Q., Marecek, J., & Chu, B. (1994). Solution behavior of buckminsterfullerene (C_{60}) in benzene. *J. Chem. Phys.*, *101*, 2665–2675.

[3] Sun, Y. P., Ma, B., Bunker, C. E., & Liu, B. (1995). All-carbon polymers (polyfullerenes) from photochemical reactions of fullerene clusters in room-temperature solvent mixtures. *J. Am. Che. Soc.*, *117*, 12705–12711.

[4] Smith, A. L., Walter, E., Korobov, M. V., & Gurvich, O. L. (1996). Some enthalpies of solution of C_{60} and C_{70}. Thermodynamics of the temperature dependence of fullerene solubility. *J. Phys. Chem.*, *100*, 6775–6780.

[5] Ahn, J. S., Suzuki, K., Iwasa, Y., & Mitani, T. (1997). Photoluminescence of C_{60} aggregates in solution. *J. Lumin.*, *72/74*, 464–466.

[6] Rudalevige, T., Francis, H., & Zand, R. (1998). Spectroscopic studies of fullerene aggregates. *J. Phys. Chem. A*, *102*, 9797–9802.

[7] Ying, Q., Marecek, J., & Chu, B. (1994). Slow aggregation of buckminsterfullerene (C_{60}) in benzene solution. *Chem. Phys. Lett. 219*, 214–218.
[8] Mrzel, A., Mertelj, A., Omerzu, A., Copic, M., & Mihailovic, D. (1999). Investigation of encapsulation and solvatochromism of fullerenes in binary solvent mixtures. *J. Phys. Chem. B*, *103*, 11256–11260.
[9] Allemand, P. A., Khemani, K. C., Koch, A., Wudl, F., Holczer, K., Donovan, S., Gruner, G., & Thompson, J. D. (1991). *Science*, *253*, 1154.
[10] Sybley, S. P., Campbell, R. L., & Silber, H. B. (1995). Solution and solid state interactions of C_{60} with substituted anilines. *J. Phys. Chem.*, *99*, 5274–5276.
[11] Ichida, M., Sohda, T., & Nakamura, A. (1999). Optical transition and ionicity of C_{60}/amine charge-transfer complexes studied by optical spectroscopy. *Chem. Phys. Lett.*, *310*, 373–378.
[12] Otto, A. (1984). Surface enhanced Raman scattering. In: *Topics in Applied Physics, Light Scattering in Solids IV*, Chang, R. K. & Furtak, T. E. (Eds.), Spinger Verlag: Berlin Vol.54.
[13] Raether, H. (1984). *Surface plasmons on smooth and rough surfaces and gratings*, Springer: Berlin.
[14] Garrell, L., Herne, T. M., Szfranski, C. A., Diederich, F., Ettle F., & Whetten, R. L. (1991). Surface-enhanced Raman spectroscopy of C_{60} on gold: evidence for symmetry reduction and perturbation of electronic structure in the adsorbed molecule. *J. Am. Chem. Soc.*, *113*, 6302–6306.
[15] Zhang, Y., Edens, G., & Weaver, M. J. (1991). Potential-dependent surface Raman spectroscopy of buckminsterfullerene films on gold: vibrational characteristics of anionic versus neutral C_{60}. *J. Am. Chem. Soc.*, *113*, 9395–9397.
[16] Chase, S. J., Bacsa, W. S., Mitch, M. G., Pilione, L. J., & Lannin, J. S. (1992). Surface-enhanced Raman scattering and photoemission of C_{60} on noble-metal surfaces. *Phys. Rev. B*, *46*, 7873–7877.
[17] Tang, Z., Cai, X., Gao, J., Mao, B., Tian, Z., Huang, R., & Zheng, L. (1999). In-situ characterization of C_{60} coalescence reaction. *Chem. Phys. Lett.*, *306*, 345–351.
[18] Lefrant, S., Baltog, I., Baibarac, M., Schreiber, J., & Chauvet, O. (2002). Modification of surface-enhanced Raman scattering spectra of single-walled carbon nanotubes as a function of nanotube film thickness. *Phys. Rev. B*, *65*, 235401–235409.
[19] Ordal, M. A., Long, L., Bell, R. J., Bell, S., Bell, R. R., Alexander, R. W., & Ward, C. A. (1983). *Appl.Opt.*, *22*, 1099.
[20] Baltog, I., Primeau, N., & Reinisch, R. (1995). Surface enhanced Raman scattering on silver grating: optimized antennalike gain of the stokes signal of 10^4; *Appl. Phys. Lett.*, *66*, 1187–1189.
[21] Dresselhauss, M. S., Dresselhauss, G., & Eklund, P. C. (1996). *Science of fullerenes and carbon nanotubes*, Academic Press: New York.
[22] Lebedkin, S., Rietchel, H., Adams, G. B., Eisler, H. J., Kappwes, M., & Kratchmer, W. (1999). Quantum molecular dynamics calculations and experimental Raman spectra confirm the proposed structure of the odd-numbered dimeric fullerene C_{119}; *J. Chem. Phys. 110*, 11768–11778.
[23] Massey, A. G., Thompson, N. R., Johnson, B. F. G., & Davis, R. (1975). *The Chemistry of Copper, Silver and Gold*, Bailar, J. C., Jr., Emeleus, H. J., Sir RonaldNyholm, F. R. S., & Trotman Dickenson, A. F. (Eds.), Pergamon Press.
[24] Garell, R. L., Heerne, T. M., Szafranski, C. A., Diederich, F., Ettl, F., & Whetten, R. L. (1991). Surface-enhanced Raman spectroscopy of C_{60} on gold: evidence for symmetry reduction and perturbation of electronic structure in the adsorbed molecule. *J. Am. Chem. Soc.*, *113*, 6302–6303.

[25] Porezag, D., Pederson, M., Frauenheim, Th., & Kohler, Th. (1995). Structure, stability, and vibrational properties of polymerized C_{60}. *Phys. Rev. B*, *52*, 14963–14970.
[26] Senyavin, V. M., Davydov, V. A., Kashevarova, L. S., Rakhmaninova, A. V., Agafonov, V., Allouchi, H., Ceolin, R., Sagon, G., & Szwarc H. (1999). Spectroscopic properties of individual pressure-polymerized phases of C_{60}. *Chem. Phys. Lett.*, *313*, 421–425.
[27] Semkin, V. N., Spitsina, N. G., & Graja, A. (1994). FT IR transmission spectral study of some single crystals of C_{60} clathrates. *Chem. Phys. Lett.*, *233*, 291–297.
[28] Adams, G. B., Page, J. B., Sankey, O. F., & O'Keefe, M. (1970). Polymerized C_{60} studied by first-principles molecular dynamics. *Phys. Rev. B*, *52*, 17471–17479.
[29] Tuinstra, F. & Koenig, J. L. (1970). *J.Chem.Phys.*, *53*, 1126–1130.
[30] Nemanich, R. J. & Solin, A. (1979). First- and second-order Raman scattering from finite-size crystals of graphite. *Phys. Rev. B*, *20*, 392–401.
[31] Kawashima, Y. & Katagiri, G. (1995). Fundamentals, overtones, and combinations in the Raman spectrum of graphite. *Phys. Rev. B*, *52*, 10053–10059.
[32] Menon, M., Subbaswamy, K. R., & Sawatarie, M. (1994). Structure and properties of C_{60} dimers by generalized tight-binding molecular dynamics. *Phys. Rev. B*, *49*, 13966–13969.